International Journal of Biological Macromolecules 224 (2023) 223–232

Contents lists available at ScienceDirect

International Journal of Biological Macromolecules

journal homepage: www.elsevier.com/locate/ijbiomac

Fabrication and in vitro evaluation of chitosan-gelatin based aceclofenac loaded scaffold

Irfa Basharat Rajput [a], Fahad Khan Tareen [b], Atif Ullah Khan [a], Naveed Ahmed [a], Muhammad Farhan Ali Khan [b], Kifayat Ullah Shah [a,*], Abbas Rahdar [c,*], Ana M. Díez-Pascual [d,*]

[a] Department of Pharmacy, Quaid-i-Azam University, Faculty of Biological Sciences, 45230 Islamabad, Pakistan
[b] Faculty of Pharmacy, Capital University of Science and Technology, Islamabad Expressway, Kahuta Road, Zone-V, Islamabad, Pakistan
[c] Department of Physics, University of Zabol, Zabol 98613-35856, Iran
[d] Universidad de Alcalá, Facultad de Ciencias, Departamento de Química Analítica, Química Física e Ingeniería Química, Ctra. Madrid-Barcelona, Km. 33.6, 28805 Alcalá de Henares, Madrid, Spain

ARTICLE INFO

Keywords:
Bio-scaffold
Chitosan
Gelatin

ABSTRACT

Scaffold development is a nascent field in drug development. The scaffolds mimic the innate microenvironment of the body. The goal of this study was to formulate a biocompatible and biodegradable scaffold, loaded with an analgesic drug, aceclofenac *(Ace)*. The bioscaffold is aimed to have optimum mechanical strength and rheology, with drug released in a sustained manner. It was prepared via chemical cross-linking method: a chitosan (CS) solution was prepared and loaded with *Ace*; gelatin (GEL) was added and the mixture was cross-linked to get a hydrogel. 20 formulations were prepared to optimize different parameters including the stirring speed, drug injection rate and crosslinker volume. The optimal formulation was selected based on the viscosity, drug solubility, homogeneity, porosity and swelling index. A very high porosity and swelling index were attained. In vitro release data showed sustained drug delivery, with effective release at physiological and slightly acidic pH. SEM analysis revealed a homogeneous microstructure with highly interconnected pores within an extended polymer matrix. FT-IR spectra confirmed the absence of polymer-drug interactions, XRD provided evidences for efficient drug entrapment within the scaffold. Rheological analysis corroborated the scaffold injectability. Mathematical models were applied to in-vitro data, and the best fit was attained with Korsmeyer-Peppas.

1. Introduction

Scaffold development is comparatively a new research field offering solution to the ailments involving degeneration or atrophy of the body organs due to any acute or chronic cause. The repair mechanism aims to stimulate body's own innate microenvironment [1]. In this study, a scaffold was prepared, loaded with aceclofenac *(Ace)* as analgesic drug for targeted effects, with intended use in defected bone tissue. Bone defects are one of the major factors causing disability not only in elderly and female population, but in young population as well. These include brittle bones due to loss of bone density, susceptibility to acute fracturing, severe pain in the bones, leading to functional disability and immobility. Age is one of the biggest contributing factors to fractures. Men above 80 are at a higher risk of such traumas while in the west, three out of four hip fractures occur in women [2]. European and Asian population are at greater risk to develop such osteopathies. Rickets affects children who are of around eighteen months of age. Osteomyelitis affects 50 % of children under the age of 5, with incidence in males twice as much as in females [3,4]. Generally, females are at a greater risk to develop bone diseases owing to variation in hormonal levels and reduced testosterone levels in their body. However, malnutrition, smoking, sedentary lifestyle, and low vitamin D levels are also major contributing factors. Risk of fracture is also associated with these bone defects. Several treatment plans that are associated with degenerative bone diseases include administration of bisphosphonates, calcium, vitamin D and calcitonin etc. [5,6], with concomitant administration of analgesics like acetaminophen, aspirin, ibuprofen and naproxen to manage the pain. These drugs besides their analgesic action, impart side effects of their own. The prolonged use of NSAIDS causes gastric irritation, leading to ulceration. Excessive use of acetaminophen can cause hepatotoxicity. Both side effects can significantly compromise the efficacy, especially due to the susceptibility of the elderly population, thus

* Corresponding authors.
E-mail addresses: kushah@qau.edu.pk (K.U. Shah), a.rahdar@uoz.ac.ir (A. Rahdar), am.diez@uah.es (A.M. Díez-Pascual).

https://doi.org/10.1016/j.ijbiomac.2022.10.118
Received 27 July 2022; Received in revised form 25 September 2022; Accepted 10 October 2022
Available online 18 October 2022

reducing the usefulness of the drug.

The development of a "bio-scaffold" to be implanted in the body to serve as a support system for tissues is the base of this research study. The most important characteristic of the scaffolds is their ability to mimic the extra cellular environment forming a three dimensional structure around the damaged tissue [7,8]. The use of a scaffold in combination with stem cells has been under research for some time, but the preparation of a scaffold in combination with a drug, thus acting as a carrier for drug delivery is relatively an unexplored area.

A similar study has been discussed by Vahedi et al. [9] which aims at using 'Infrapatellar Fat Pad-Derived Mesenchymal Stem Cells' for the regeneration of articular cartilage in conditions like osteoarthritis. Another study explores the tissue healing properties of curcumin loaded in nano-scaffolds as a new type of drug delivery system to improve its biological activities as well as the scaffold functionality and efficiency [10].

The aim of this study was to develop a bio-scaffold, in injectable form, loaded with *Ace*. The polymers used were chitosan and gelatin, both of which are biocompatible and biodegradable. They are metabolized into non-toxic metabolites to be excreted out of the body [11–13]. Chitosan and gelatin have already been used to prepare scaffolds in the form of bone implants. Both polymers have been proved to be bioactive by helping in regrowth of bone and tissues [14,15]. Besides, gelatin has also been shown to increase the accumulation of fibroblasts and increase the bone mass density [16,17].

The selection of *Ace* was carried out based on several parameters. Its side effect profile for inducing peptic ulcer and gastrointestinal bleeding is much better than its counterparts. Besides it is chondroprotective in nature and inhibits effect of degrading metalloproteinases [18]. *Ace* belongs to biological classification system (BCS) class II, which means that it has low solubility and high permeability profile.

The prepared scaffold is in injectable hydrogel form. Hydrogels can be prepared by several methods, depending on the nature of the ingredients used and the application of the hydrogel. For instance, physical methods include hydrophobic interactions, complex coacervation, ionic interactions, hydrogen bonding and so forth. Conversely, chemical methods include chemical cross linking, enzyme cross linking, free radical polymerization etc. [19]. ,Chemical cross linking method was utilized herein. With its shear-thinning properties, the gel is expected to be injectable when external pressure is applied and revert to its original form when pressure is removed. This could be achieved by using a suitable syringe system. Deformities of irregular shape can also be easily accessible. The polymer, drug and cross linker concentration were modified to achieve an optimal formulation with the required amount of drug loaded and the optimum rheology. The characterization performed on the optimized formulation proved the lack of interactions between the drug and the polymers, with sustained drug release in the required period.

2. Materials and methods

2.1. Materials

Chitosan (CS), $C_{18}H_{35}N_3O_{13}$, with a medium molecular weight (190,000–310,000 Da) and degree of deacetylation in the range of 75–85 %, polyethylene glycol sorbitan monooleate (Tween 80), $C_{64}H_{124}O_{26}$, with a micellar average molecular weight of 79,000 Da, glutaraldehyde (GTA) solution (25 % w/v in water), $C_5H_8O_2$, with a molecular weight of 110.12 g/mol and gelatin (GEL) $C_{102}H_{151}N_{31}O_{39}$, Type A (300 Bloom), with an average molecular weight of 220 kDa, were obtained from Sigma Aldrich. Aceclofenac (*Ace*), [(2-{2,6-dichlorophenyl) amino} phenylacetooxyacetic acid], $C_{16}H_{13}Cl_2NO_4$, was gifted by Global Pharmaceuticals, Islamabad. Methanol, $KHPO_4$ (Potassium hydrogen phosphate), Na_2HPO_4 (disodium hydrogen phosphate), NaCl (sodium chloride) and HCl (hydrochloric acid) were purchased from BDH laboratories supplies. NaOH (Sodium hydroxide) was obtained from local suppliers.

2.2. Methods

2.2.1. Preparation of the blank scaffold

The required amounts of chemicals were weighed using an analytical balance (Ohaus PA214C). 2.5 mL of 2 % CS solution was prepared in 1 % acetic acid, by stirring for 12 h using a hotplate multi stirrer (MAGIK-MG-855). 3 % (*v*/v) Tween 80 solution was added and stirred for 1 h. Separately, 2.5 ml of 4 % gelatin solution was prepared in distilled water and added slowly to the CS solution, followed by stirring for 12 h at 37 °C. A homogeneous solution of transparent pale-white color was obtained. Then, 0.2 % v/v GTA was added as a cross linker and allowed to stir for 3 h. A pale white to pale yellow hydrogel was obtained.

2.2.2. Preparation of the drug loaded scaffold

The drug-loaded scaffold was prepared following the same process, with 15 mg of the drug being first solubilized in 0.5–1 mL of methanol and then added dropwise to the CS-Tween 80 solution, keeping the rest of the procedure the same. Sonication of the sample was performed using a Elma Sonic E-60H bath sonicator (Elma GmbH, Singen, Germany) when it was necessary to enhance the dissolution.

2.2.3. Optimization of the process parameters

Multiple parameters that influence the rheology and extent of drug dissolution in the formulation were investigated and optimized. The stirring speed was modified from 2000 to 4000 rpm. Similarly, the rate of addition of the drug solution was varied from 0.01 to 0.05 mL/min. Different percentages of the cross linker were tested, including 0.1, 0.15, 0.2, 0.25 and 0.3 %. The formulation was optimized based on the homogeneity, viscosity, and the extent of drug dissolution.

2.3. Characterization of the scaffold

2.3.1. Physical examination

The hydrogel (5 mL) was inspected visually and rubbed between the fingers to check for homogeneity and absence of grittiness [20].

2.3.2. Moisture loss, porosity and swelling ratio

The moisture content of the scaffold was determined by taking a measured amount of sample in a pre-weighed petri dish and placing it in a Memmert UN110 heating oven (Memmert GmbH, Schwabach, Germany) at 50 °C and then weighed at intervals of 12 h until the weight became constant [20]. Eq. (1) was used to determine the moisture loss.

$$\text{Moisture loss } (\%) = \frac{W_2 - W_1}{W2} \times 100 \quad (1)$$

Where W_1 and W_2 are the weight of the sample before and after immersion, respectively.

The liquid displacement method was used to determine the porosity. A scaffold weighing from 0.5 to 1.18 g was immersed in a graduated cylinder filled with 25 mL of distilled water for 24 h. The sample was then freeze dried and the final weight and volume were recorded [21,22]. Porosity was calculated using Eq. (2).

$$\textbf{Porosity } (\%) = \frac{\mathbf{W_2 - W_1}}{\boldsymbol{\rho} \mathbf{V_s}} \times \mathbf{100} \quad (2)$$

Where W_1 and W_2 are the weight of the sample before and after immersion, ρ is the density of distilled water and V_s is the volume of the gel after lyophilization.

The swelling index was calculated by taking a pre-weighed sample of 1.18 g and immersed in PBS 7.4 and 6.8 at 37 °C for 48 h. Excess of water was removed from the sample and weighed again [22]. Eq. (3) was used to determine the swelling ratio.

$$\textbf{Swelling}\textit{index}\ (\%) = \frac{\mathbf{W_w - W_d}}{\mathbf{W_d}} \times 100 \quad (3)$$

Where W_d is the dry weight of the scaffold (before immersion) and W_w is the wet weight of the scaffold (after immersion). All the experiments were performed in triplicate and the mean values are reported.

2.3.3. pH and rheology

2.5 g of the prepared formulation were placed in a beaker containing 25 mL of distilled water. pH was measured using a pH meter (ST Series Pen meter, IP 67 Waterproof) [23].

The rheological properties were determined using a DV-1Brookfield cone and plate viscometer (Brookfield Engineering Laboratories, MA, USA). The shear rate was set at 4, 8, 12, 16, 20, 24, 28 and 32 rpm, to determine the thixotropic behavior of the scaffold [19].

2.3.4. Drug content uniformity test

Drug content uniformity test was carried out in order to make sure about the uniform dispersion of the drug. For such purpose, 2 mL of the formulation were transferred to a beaker with 20 mL of methanol, and the mixture was stirred for 2 h. The volume was made up to 100 mL and filtered with a 0.45 μm Multipore filter [24]. The absorbance was measured at 275 nm with a Halo DB-20 UV–Vis double beam spectrophotometer (Dynamica Scientific Ltd., Livingston, UK) and the drug content was determined using a standard curve with R^2 value of 0.999. The experiment was repeated three times and the mean value was calculated. Eq. (4) was used to determine the percentage of drug content.

$$\textbf{Drug}\textit{content}\ (\%) = \frac{\textbf{Amountofdrug}\textit{detected}}{\textbf{Amountofdrug}\textit{loaded}} \times \mathbf{100} \quad (4)$$

2.3.5. Polydispersity index (PDI) and zeta potential

To determine the homogeneity of the formulation, PDI was measured by diluting 10 μl of the formulation in 1 mL of distilled water, using a Nano ZS-90 Zeta Sizer (Malvern, Worcestershire, UK). Zeta potential was measured to assess the extent of dispersion and the absence of agglomeration in the formulation.

2.3.6. Fourier Transform Infrared Spectroscopy (FT-IR)

FT-IR was used to confirm the absence of interactions between the polymers and the drug molecules. A Spectrum100 FT-IR Spectrophotometer (*Perkin Elmer*, Waltham, MA, USA) was used to perform transmission measurements on CS, GEL, *Ace* and the lyophilized form of the final formulation, in the wavenumber range of 4000–5000 cm^{-1}.

2.3.7. X-ray diffraction (XRD)

The crystalline structure of the samples was analyzed via XRD technique with a PW1730 diffractometer (Philips, Eindhoven, Netherlands). XRD of the lyophilized final formulation was recorded in the 2Θ range between 10 and 80°, at a scan speed of 0.5°/s, to check the conversion of the drug from the crystalline to the amorphous form.

2.3.8. Scanning Electron Microscopy (SEM)

The surface morphology and pore size of the samples were analyzed by SEM using a VEGA3 high-performance analytical microscope (Tescan, Brno, Czech Republic). Prior to the analysis, 10 μl of the formulation were diluted 100 times and sonicated for 15 min. A small volume of the diluted formulation was deposited on a glass slide, dried thoroughly and then coated with gold using a sputter coater to avoid charging during electron irradiation.

2.3.9. In vitro drug release

In vitro drug release was performed on the prepared scaffold and the formulation at pH 7.4 and 6.8, using dialysis bag diffusion technique. Phosphate buffer solutions (PBS) were used to mimic the physiological environment of the body under both normal and inflammatory conditions. Each formulation containing the same amount of drug was placed in a dialysis bag and immersed in the beakers containing PBS (pH 7.4 and 6.8). All the beakers were placed in a Memmert SV-1422 shaking bath (Memmert GmbH, Schwabach, Germany) at 100 rpm and 37 °C. The dialysis bag acted as the donor compartment, while the beaker containing the PBS as receptor compartment. At specified time intervals of 0.25, 0.5, 0.75, 1, 2, 3, 4, 6, 8, 12, 18, 24, 48 and 72 h, 1 mL of the samples was separated to measure the drug release. The sample volume removed was continuously replaced with fresh PBS, to maintain the sink conditions. Identical procedure was applied for the formulation, at pH 7.4 and 6.8. The absorbance of the samples was measured on a UV–Vis spectrophotometer (Dynamica Scientific Ltd., Livingston, UK) and the percentage of cumulative release was calculated at each pH.

2.3.10. Drug release kinetics

The data collected from the in vitro drug release assay was analyzed to determine the mechanism of drug release from the formulation. Several mathematical models including zero order, first order, Higuchi, Hixon Crowell and Korsmeyer Peppas were applied to calculate the amount of drug released as a function of time. The correlation coefficient (R^2) was obtained for each model and that with the highest value was selected in order to explain the drug release behavior.

2.3.11. Stability of the scaffold

Accelerated stability studies were carried out using ICH guidelines, at 40 ± 2 °C and relative humidity of 75 ± 5 % [25]. The scaffold was examined by physical parameters (color, homogeneity, and grittiness), pH, extent of sedimentation and drug content.

3. Results

3.1. Optimization of the scaffold

For optimization, a total of 20 formulations were developed (Table 1), and were examined for physical appearance and rheological properties. The CS:GEL ratio was fixed at 1:2. Increasing amounts of drug were loaded in the scaffold to determine the maximum amount that can be loaded. The percentage of cross linker added was a crucial parameter. As can be concluded from Table 1, F11 shows the most promising characteristics in terms of physical appearance, drug solubility and rheological properties.

3.2. Impact of the parameters on the final formulation

The CS:GEL ratio is crucial to attain an optimum swelling and porosity of the scaffold. It is also an important parameter that determines the final viscosity and thus the mechanical properties of the scaffold. Similarly, the amount of cross linker used is a key parameter since it determines the rheology and hence the injectable nature of the final formulation. The use of a cross linker percentage higher than the optimum turned the formulation into semi solid form, thus reducing its ease of injection. The drug loading capacity of the scaffold was determined by gradually increasing the amount of drug from a minimum value of 5 mg to maximum of 20 mg at which sedimentation occurs, and the drug is insoluble in the scaffold. Thus, 15 mg was chosen as the optimum amount of drug loaded in the scaffold.

3.3. Optimization of the process parameters

During the preparation of the formulations, several parameters that influence the viscosity of the scaffold and the extent of drug dissolution were studied (Table 1). These parameters include the stirring speed, the drug injection rate and the cross linker volume. Different values for these parameters were tested in order to obtain the most suitable formulation (Table 1).

Table 1
Optimization of Ace loaded scaffold.

Formulation	Stirring Speed (rpm)	Injection rate (mL/min)	Drug Concentration (mg)	Cross Linker (% v/v)	Viscosity at 50 rpm (cp)	Physical Appearance
F1	2000	0.01	5	0.1	39.69	Liquid
F2	2000	0.01	10	0.1	35.4	Liquid
F3	2000	0.01	15	0.1	40.7	Liquid
F4	2000	0.01	20	0.1	42.8	Liquid + Sedimentation
F5	2500	0.02	5	0.15	50.1	Semi liquid gel
F6	2500	0.02	10	0.15	55.7	Semi liquid gel
F7	2500	0.02	15	0.15	60.2	Semi liquid gel
F8	2500	0.02	20	0.15	61.8	Semi liquid gel + Sedimentation
F9	3000	0.03	5	0.2	80.6	Homogenous gel+ no Sedimentation
F10	3000	0.03	10	0.2	85.7	Homogenous gel+ no Sedimentation
F11	3000	0.03	15	0.2	87.61	Homogenous gel+ no Sedimentation
F12	3000	0.03	20	0.2	85.1	Homogenous gel+ Sedimentation
F13	3500	0.04	5	0.25	110.6	Viscous gel
F14	3500	0.04	10	0.25	115.21	Viscous gel
F15	3500	0.04	15	0.25	120.5	Viscous gel
F16	3500	0.04	20	0.25	110.4	Viscous gel + Sedimentation
F17	4000	0.05	5	0.3	120.8	Semi solid gel
F18	4000	0.05	10	0.3	120.4	Semi solid gel
F19	4000	0.05	15	0.3	115.7	Semi solid gel
F20	4000	0.05	20	0.3	125.4	Semi solid gel + Sedimentation

3.3.1. Stirring speed

Stirring speeds slower than the optimum led to reduced drug and cross linker solubility, thus resulting in non-homogeneous formulations (Table 1). On the other hand, stirring speeds faster than the optimum led to frothing, which influenced the solubility of the drug and the cross linker.

3.3.2. Injection rate

The drug was dissolved in 1 mL of methanol and slowly injected into the CS and Tween 80 solution. An injection rate of 0.03 ml/min was found to be optimal (Table 1).

3.3.3. Cross linker volume

The cross linker volume was found to be the most important parameter (Table 1). A small cross linker volume led to reduced viscosity while a high cross linker volume turned the formulation into semi-solid form. Based on the final physical appearance, rheological properties, and the drug solubility, F11 was chosen as the optimal formulation.

3.4. Characterization of the scaffold

3.4.1. Physical examination

The color of the scaffold ranged from off-white to pale yellow. It was

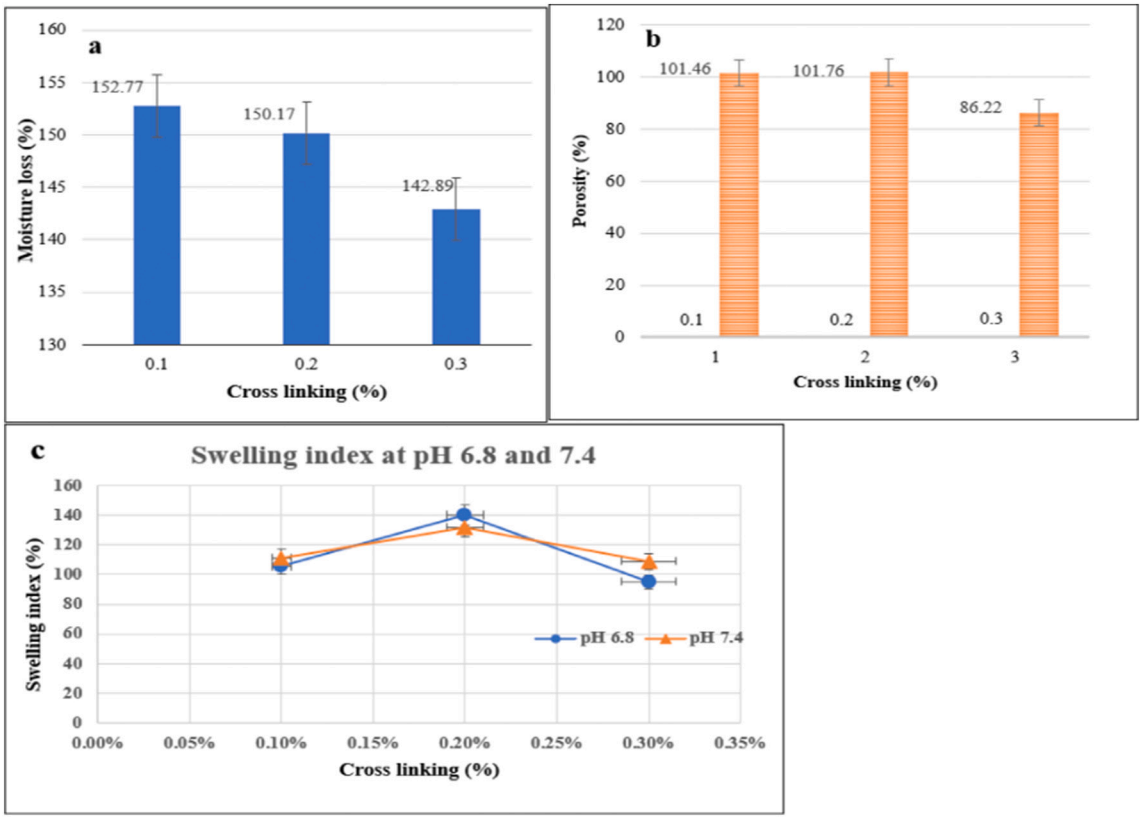

Fig. 3.1. Comparison of the moisture loss (a), porosity (b) and swelling index at pH 6.8 and 7.4 (c) of the 0.1, 0.2 and 0.3 % cross linked scaffolds.

in semi-solid gel form and was viscous in nature. Upon rubbing between the fingers, the consistency was found to be smooth and non-gritty.

3.4.2. Moisture loss, porosity and swelling ratio

The mean percentage of moisture loss calculated following Eq. (1) was found to be 152.77 ± 2.76 % for the 0.1 % cross linked sample, while for the 0.2 and 0.3 % cross linked samples, the moisture content was 150.17 ± 2.59 % and 142.89 ± 1.42 % respectively, as shown in Fig. 3.1(a). The highest moisture loss was for the 0.1 % cross linked sample while the lowest for the 0.3 % one, in agreement with previous studies on CS/GEL/PVA hydrogels [22].

Porosity is an important evaluation index for tissue-engineered scaffold materials. The mean porosity of the samples containing 0.1, 0.2 and 0.3 % cross linker calculated using Eq. (2) was found to be 101.46 ± 2.08, 101.76 ± 1.93, and 86.22 % ± 3.16 %, respectively, as shown in Fig. 3.1(b). Interestingly, both 0.1 and 0.2 % cross linked scaffolds show very close percentages of porosity: also, there is a clear overlap of their error bars, which indicates that the difference is not statistically significant. However, the 0.2 % cross linked one was selected due to its superior rheological behavior. It is worthy to note that the values obtained herein are higher than those reported for polymer hydrogel-based scaffolds whose porosity is typically below 85 % [26].

The mean degree of swelling was calculated using Eq. (3), and the results are compared in Fig. 3.1(c). The samples prepared herein showed very good swelling behavior since CS and GEL are hydrophilic polymers. The highest swelling percentages (140.16 % in PBS at pH 6.8 and 131.93 % in PBS at pH 7.4) were found for the 0.2 % cross linked sample. The 0.1 and 0.3 % cross linked formulations showed somewhat less degree of swelling i.e., 105.83 and 111.37 % in PBS at pH 6.8 and 95.15 and 108.92 % in PBS at pH 7.4, respectively.

3.4.3. pH and rheology

The pH of the scaffolds was measured in triplicate and the mean value was found to be 7.16 ± 0.12. This value is close to the physiological pH, with a slight shift towards acidic range, which may be due to the acidic nature of CS solution. Fig. 3.2(a) shows the injectable nature of the scaffold and Fig. 3.2(b) reveals that the scaffold reverts to its original gel like viscosity after the external pressure is removed.

The room temperature rheological properties of the optimized formulation were determined, which showed shear thinning behavior, i.e., a decrease in viscosity with the increase in shear rate, as can be observed in Fig. 3.2(c). It has been reported that shear thinning is caused by the disentanglement of polymer chains during flow. At rest, the polymeric chains of the hydrogel are entangled and randomly oriented. However, when undergoing agitation at a high enough rate, these highly anisotropic polymer chains start to disentangle and align along the direction of the shear force, leading to less interaction and a larger amount of free space, exhibiting subsequent decreased viscosity [19].

3.4.4. Drug content uniformity

Drug content uniformity test was performed to get a more reliable measurement of the amount of drug in the solution. The mean drug content of three samples was calculated to be 81.63 ± 0.06 %.

3.4.5. Polydispersity index (PDI) and zeta potential

Polydispersity characterization is essential since it is difficult to control sample-wide uniformity for the successful design, formulation and development of nanosystems for pharmaceutical applications. The drug loaded scaffold showed a unimodal peak with a mean particle size of 272.5 nm and a PDI value of 0.399, as shown in Fig. 3.3(a). This corroborates the homogeneity of the formulation. The value obtained

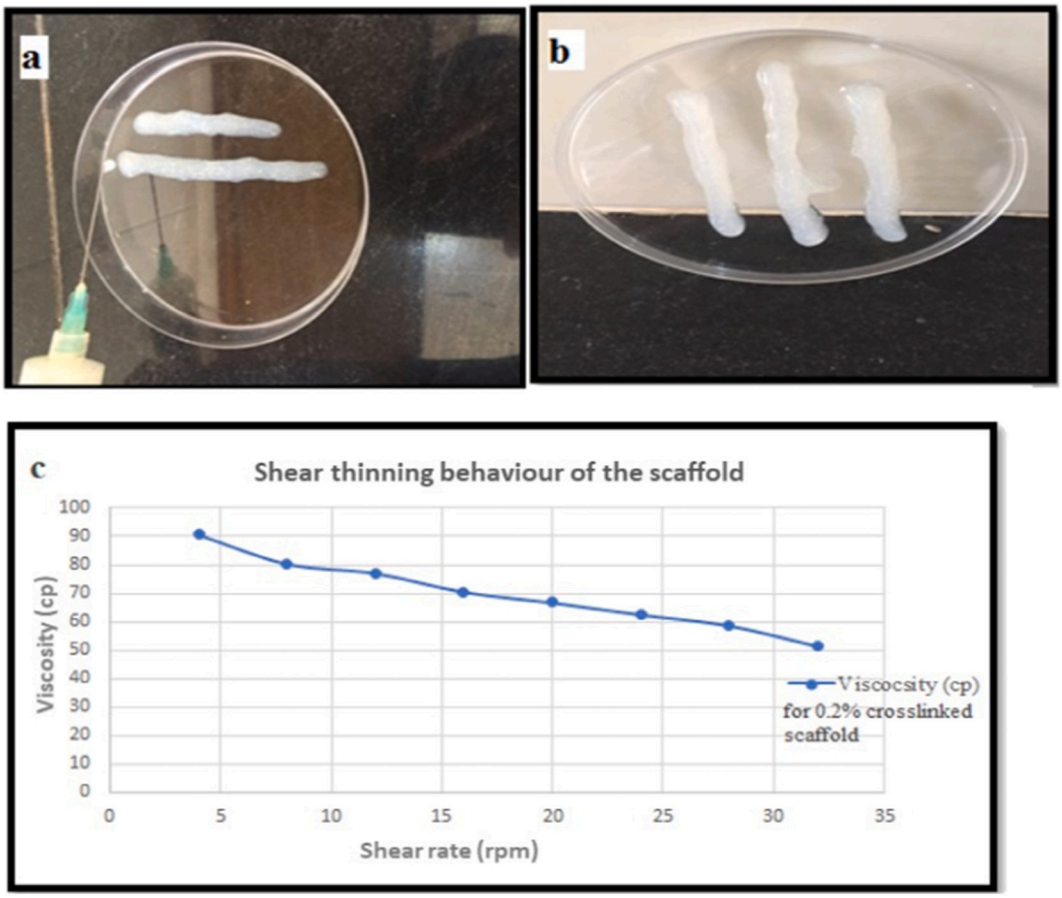

Fig. 3.2. (a) Injectable nature of the scaffold; (b) The scaffold reverts to the gel form after removing the external pressure; (c) Shear thinning behavior of the scaffold.

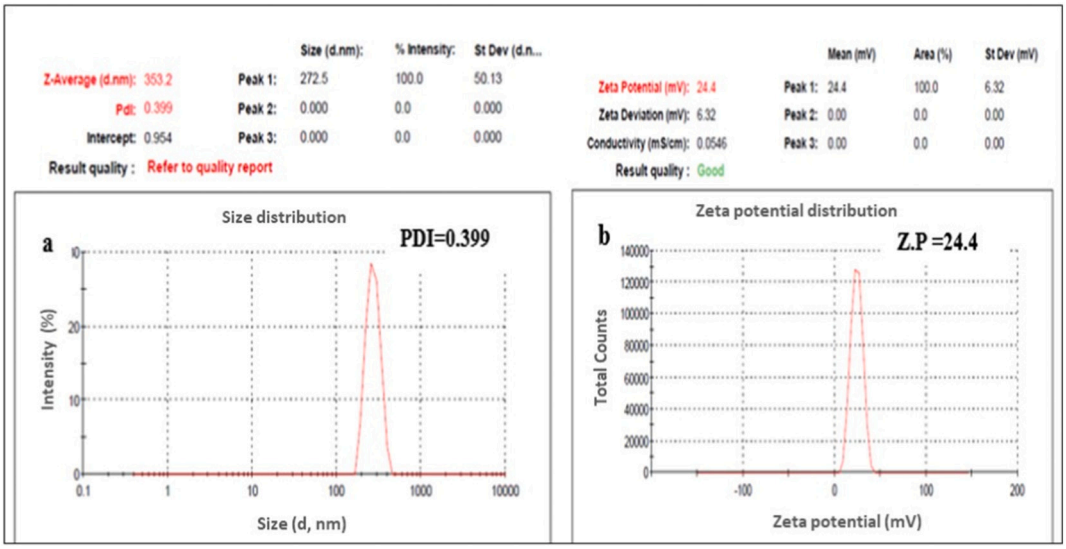

Fig. 3.3. (a) Particle size distribution and (b) zeta potential of the optimized formulation.

lies within the accepted range for biological polymers.

The zeta potential shows the surface charge of particulate formulations, and is related to their colloidal stability. Higher zeta potential values prevent aggregation due to electrostatic repulsion between similarly charged particles, thus conferring stability to colloidal dispersions. The value of zeta potential for the formulation was found to be 24.4 mV, with a unimodal peak as shown in Fig. 3.3(b), indicating the electro kinetic stability [27,28].

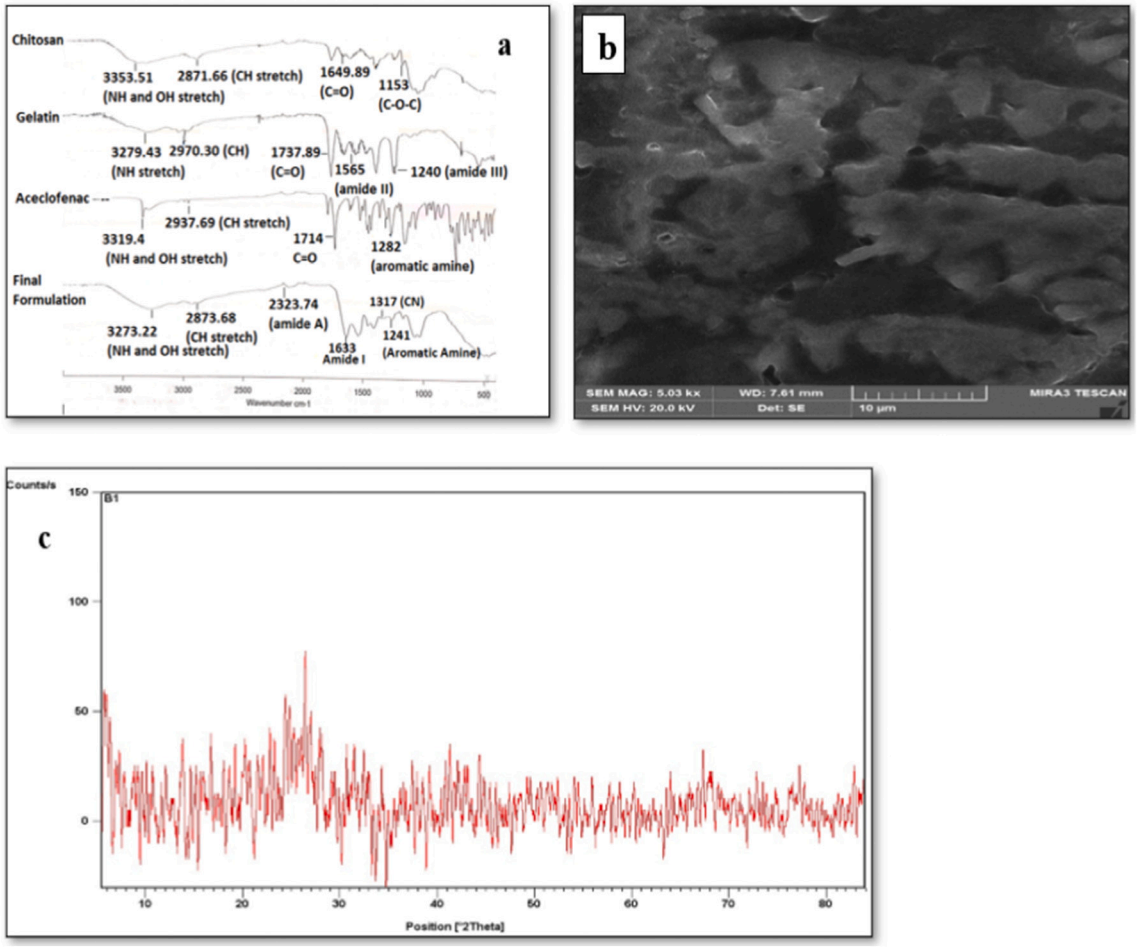

Fig. 3.4. (a) FT-IR spectrum of CS, GEL, Ace and the final formulation; (b) SEM image showing the porous nature of the scaffold with an extended polymeric network; (c) XRD of the final formulation.

3.4.6. Fourier Transform Infrared spectroscopy (FT-IR)

The neat polymers (GEL and CS), the pure drug and the final formulation were analyzed using FT-IR, and their spectra are compared in Fig. 3.4(a). The characteristic peaks of all the materials used were observed in the final formulation. N—H and O—H stretching vibrations were observed at 3273 cm^{-1}, and C—H stretching vibrations were found at 2929 and 2873 cm^{-1}, which can also be observed in the spectra of the neat polymers and the drug. Peaks for GEL were observed at 2324 cm^{-1} (amide A band), 1539 cm^{-1} (N—H bending of amide II) and 1402 cm^{-1} (CH_2 bending) [29–31]. The peak observed at 1633 cm^{-1} (C═O stretching of amide I) is common for both GEL and CS. Besides, the peak at 1317 cm^{-1} in the spectrum of CS corresponds to the C—N stretching of amide III, the absorption band at 1153 cm^{-1} can be attributed to the asymmetric stretching of the C-O-C bridge and the bands at 1066 and 1028 cm^{-1} correspond to C—O stretching vibrations. Similarly the characteristic peaks of *Ace* were observed, including the C—N stretching of aromatic amines at 1281 cm^{-1}, and that at 1452 cm^{-1} due to C—C stretching vibrations of the aromatic ring [32]. The minor shifts in the wavenumbers observed could be attributed to the cross linking between the polymers. Overall, FT-IR spectroscopy confirmed the presence of the characteristic functional groups of each component in the final formulation and the absence of interactions among them.

3.4.7. Scanning electron microscopy (SEM)

The SEM image of the scaffold shown in Fig. 3.4 (b) reveals a homogeneous microstructure with highly interconnected pores within an extended polymer matrix, in agreement with observations from previous works on biopolymer hydrogels [26]. The addition of Tween 80 surfactant avoided polymer aggregation. The absence of delamination in the gel matrix indicates the lack of interactions between the drug molecules and the polymer matrix [33,34]. The pore size, as observed in the image, lies in the range of 10–20 μm. These characteristics are reported to be optimum to provide the required mechanical stability and viscosity to allow the proliferation of cells [14].

3.4.8. X-ray Diffraction (XRD)

XRD of the final formulation showed reduced intensity of the peaks of the drug at 2θ values of 18.5, 19.1, 22, 23.9, 25 and 26°, as shown in Fig. 3.4(c). The most plausible explanation is the entrapment of the drug molecules within the polymer matrix, along with its conversion from crystalline to amorphous nature by size reduction, thus masking the peaks of the drug.

3.4.9. In vitro drug release

The in vitro drug release data at pH 7.4 showed a significant drug delivery from the optimal scaffold formulation developed herein, i.e., near to 20 % in a sustained release fashion in 72 h, while almost the entire drug was released from the marketed formulation in around 5 h, as shown in Fig. 3.5(a). At pH 6.8, the amount of drug released by the scaffold formulation was around 30 %, while for immediate release marketed formulation, nearly all the drug was released within 4–5 h, as shown in Fig. 3.5 (b). Calibration curves of the experimental data at both pH 7.4 and 6.8 yield R^2 values of 0.999.

3.4.10. Kinetic models

The drug release data from the scaffold at pH 7.4 and 6.8 were analyzed using mathematical models. Among zero order, first order, Higuchi, Korsmeyer-Peppas and Hixon Crowell, the best fit model was selected based on the value of the correlation coefficient (R^2). The maximum value of R^2 was 0.8528 and 0.9851 for pH 7.4 and 6.8, respectively, for Korsmeyer–Peppas model. The value of the release exponent (n) was 0.467 and 0.559 for pH 7.4 and 6.8, respectively, which reveals that the drug delivery follows a non-Fickian diffusion mode. The deviation from the Fickian behavior may be attributed to the drug release controlled not only by a single mechanism but by both the degradation and swelling of the polymers [35].

3.4.11. Stability studies

Stability studies were carried out to ensure that the developed formulation remains stable throughout the requested shelf life, and that it does not undergo any major physical or chemical change. The results of the stability studies are shown as in Table 2.

Table 2
Accelerated stability studies of the developed scaffold.

Time (months)	Phase Separation	Color change	Grittiness	pH	Drug content
0	No	No color change	No	7.23 ± 0.05	81.98 ± 1.68 %
1	No	No color change	No	7.2 ± 0.1	81.05 ± 0.95 %
3	No	No color change	No	7.06 ± 0.05	80.77 ± 1.36 %

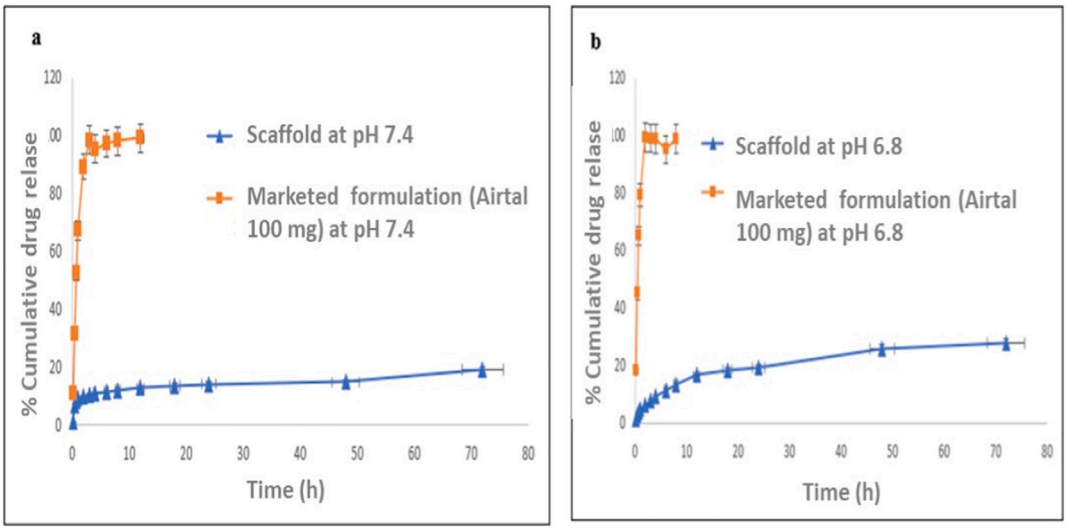

Fig. 3.5. Comparison of the percentage cumulative release of drug from the scaffold formulation developed and the marketed formulation (a) at pH 7.4 ($p < 0.0001$); (b) at pH 6.8 ($p < 0.0001$).

4. Discussion

The scaffold has been designed to be injectable with shear thinning property. The polymers employed are biocompatible and biodegradable. Less dose of *Ace* is used than oral, thus aimed at reducing side effects of oral intake. The release of *Ace* from the scaffold in sustained manner can be interpreted as prolonged effect.

The scaffold is of gel like consistency with homogeneity throughout. Its uniform and smooth nature indicates the equal distribution of the drug in the formulation. The high moisture content of the scaffold corroborates its large capacity to hold water, which is important to attain the optimum viscosity and mechanical properties. The porosity percentage was found to be near 100 % [36]. Such high water content and porosity are crucial for the diffusion and degradation of the polymer, and enable the sustained drug release from the scaffold.

The pH of the scaffold is within the physiological range, though slightly shifted towards to the acidic side. This pH shift results in improved drug release, given that in osteopathic conditions, the pH of the tissues is somewhat acidic. Besides, this lowering of pH aids to attract the inflammatory mediators and mesenchymal stem cells at the site of injury [37]. Additionally, *Ace* shows improved release profile at pH 6.8 compared to 7.4 [38]. This is also corroborated by the release data, which demonstrated that the drug delivery from the scaffold is better at acidic pH than at physiological pH.

The scaffold shows shear thinning behavior, i.e., becomes liquid when a external pressure is applied, and is reverts to its gel form when the external pressure is removed. This rheological behavior aids in making the formulation "injectable" when the viscosity of the scaffold is reduced by applying an external pressure and reverts to its original viscosity when the external force is removed.

The zeta potential and PDI corroborate the homogeneity and stability of the system. The PDI value obtained of 0.399 confirms the minimum aggregation of the polymer particles, ascribed to the presence of the surfactant. Similarly, the zeta potential value of 24.4 mV indicates the electro-kinetic stability of the scaffold. This demonstrates the absence of floccules in the gel matrix, and thus the stability of the developed system.

The XRD of the scaffold corroborates the amorphous nature of the drug due to the decreased intensity of the peaks. This suggests encapsulation of the drug in the hydrogel matrix. The presence of the characteristic peaks of the polymers and the drug in the FT-IR spectrum of the final formulation indicate that the molecular structures of the polymers and the drug are intact. This indicates that the drug and the polymers will not lose their therapeutic and physicochemical effects, respectively. However, minor shifts in the position of the peaks can be observed, which could be attributed to cross linking between the chitosan and the gelatin.

SEM images of the scaffold showed a homogeneous microstructure with highly interconnected pores within an extended matrix of polymers in gel, The pore size was estimated to be around 10–20 μm, as stated in the results section, which falls in the category of microporosity. Both are very important for the efficient functioning of the scaffold [39]. Pores are important for the interaction of the extracellular fluid with the scaffold, thus facilitating the drug release. Besides, micropores <10 μm are useful for ion exchange and protein adsorption. Former studies [40–42] have shown that pore sizes of <100 μm are helpful in forming non-mineralized osteoid tissue. A study carried out by Kong et al. [43] has also shown that a pore size in the range of 15–40 μm helps in increasing the mechanical strength of the bone. Besides, porosity also has the role of providing optimum rheological properties to the scaffold.

The in vitro drug release of the developed scaffold and an immediate release marketed formulation were investigated both at 7.4 (physiological pH) and at a slightly acidic pH (6.8), which mimics the acidic environment in inflammatory conditions. The drug release from the marketed formulation was almost immediate for both pH, while the delivery from the scaffold was slow and in a sustained manner, and was significantly higher at an acidic pH compared to the physiological pH, thus indicating the efficiency of the scaffold.

The mathematical models applied to the release data show that the best fit was obtained using Korsmeyer-Peppas, which yield to the highest R^2 value (0.8528 and 0.9851 for pH 7.4 and 6.8, respectively). The value of 'n' (0.467 and 0.559 for pH 7.4 and 6.8, respectively) show that the drug release from the scaffold follows a non-Fickian behavior, occurring by both diffusion and degradation.

5. Conclusions

The current study focused on the development and in vitro evaluation of a bioscaffold comprising gelatin and chitosan polymers loaded with an analgesic drug *(Ace),* with the aim to attain optimum physical, mechanical and rheological properties. Numerous formulations were prepared, which were evaluated for different parameters including the stirring speed, the drug injection rate and the cross linker volume. The optimal formulation was chosen based on the viscosity, drug solubility, homogeneity, porosity and swelling index. In vitro studies showed drug release in a sustained manner, which was effective both at physiological and slightly acidic pH. Different theoretical models were applied to describe the experimental data, and the best fit was attained with Korsmeyer-Peppas.

SEM analysis revealed a uniform microstructure with highly interconnected pores within an extended polymer matrix. FT-IR, XRD and rheological analyses corroborated the absence of interactions between the biopolymers and the drug, the successful drug entrapment within the scaffold and its injectability, respectively. The optimal formulation developed herein is suitable to be used in various anatomical sites due to its flexible rheological properties. Besides, the preparation method is simple, straightforward and thus easily reproducible. Another benefit is its cost effectiveness, due to the use of cheap components for the synthesis.

6. Future prospects

The work reported herein proposes an innovative formulation of a hydrogel scaffold loaded with a drug. It is a pilot study with a complete analysis of the pharmacological kinetics of the novel formulation. However, with a view to use the developed scaffold for drug delivery applications, it is of crucial importance to test it in living systems; that is, in order to testify the safe reliability and drug delivery ability of the developed hydrogel for clinical applications, a series of biological studies need to be carried out. These evaluations would follow the guidelines and harmonized practices reported in previous studies that investigated novel hydrogel drug delivery systems [44–46]. In this regard, animal experiments including magnetic resonance imaging, in vivo photothermal assay and in vivo biodistribution analysis would be performed. Besides, the potential chronic toxicity of the developed formulation needs to assessed, in order to characterize potential adverse effects following its repeated administration. Therefore, future prospects of this study include the ex vivo and in vivo analysis to evaluate toxicological concerns and pharmacokinetic profile.

In addition to gelatin and chitosan, a number of natural and synthetic polymers with low toxicity and high biodegradability are available to develop hydrogel scaffolds. Collagen, alginate, methylcellulose, polydopamine and hyaluronic acid are good candidates as natural products [47], while poly lactic acid (PLA), polyglycolic acid (PGA), poly(lactic-co-glycolic acid) (PLGA), polycaprolactone (PCL), polyacrylic acid (PAA), polyethylene glycol (PEG), poly vinyl alcohol (PVA), poly(2-hydroxyethyl methacrylate) (pHEMA) and poly (N-vinylcaprolactam) (PNVCL) are some biodegradable synthetic agents [48,49]. Novel perspectives focus on the research of new biopolymers compatible with hydrogel technology [50]. In this regard, bacterial biopolymers show great potential including bacterial polyesters like polyhydroxyalcanoates, and bacterial polysaccharides including xanthan

gum, scleroglucan, gellan gum, curdlan, bacterial alginate, dextran, pullulan, bacterial cellulose and so forth. In addition to polypeptides and polysaccharides being capable of forming hydrogels, a mixture of them can also be used to design new gel compounds [51]. For instance, the extracellular matrix (ECM) comprises both fibrous proteins and a polysaccharide called glycosaminoglycans, and can form scaffolds with adjustable gelation kinetics. Besides, DNA crosslinked hydrogels are a key tool for drug delivery due to their porosity, biocompatibility, and ability to lay out the DNA sequence via customized programmes [51]. DNA-based hydrogels are an effective solution since they are an affordable, programmable, and sensitive platform for biosensing. The ability of DNA hydrogels to biosense, scaffold, and drug deliver makes them a superior candidate for novel cancer therapeutics [52].

Despite the present study focuses on the macromolecular aspects of the scaffold, for future research, it can be modified to incorporate novel aspects of nanomedicine to attain more efficiency. In this regard, polymeric NPs, dendrimers, micelles, liposomes and niosomes are being considered in designing targeted drug delivery systems [53]. The aforementioned nanostructures can effectively encapsulate and release various hydrophobic/hydrophilic therapeutic molecules including drugs and prodrugs in a sustained manner. Since they show nanoscale dimensions, they can enhance the therapeutic efficacy of bioactive molecules, allowing them to accumulate preferentially at the target site. In particular, drugs with poor solubility and low absorption ability can be tagged with these nanostructures. Furthermore, these nanomaterials can protect the encapsulated drug from degradation, thereby increasing its therapeutic value and reducing systemic toxicity. However, the NP efficiency depends on many factors including the size, shape, and other inherent biophysical/chemical properties. For instance, synthetic polymeric NPs of PVA, PEG, PLA, PGLA, and so forth with diameters in the range of 10 to 1000 nm show ideal characteristics to be used as efficient delivery vehicles due to their high biocompatibility and biodegradability [54]. The incorporation of such NPs in the scaffold developed herein can be a potential subject for further investigations. This study opens new horizons for future research in lesser explored areas using drug loaded scaffolds.

Funding

Financial support from the Community of Madrid within the framework of the multi-year agreement with the University of Alcalá in the line of action “Stimulus to Excellence for Permanent University Professors”, Ref. EPU-INV/2020/012, is gratefully acknowledged.

CRediT authorship contribution statement

Irfa Basharat Rajput: Methodology, Data curation, Writing- Original draft preparation. **Fahad Khan Tareen**: Investigation, Software, Validation; Writing- Reviewing and Editing. Atif Ullah Khan: Data curation, Writing- Original draft preparation. **Naveed Ahmed:** Methodology, Writing- Original draft preparation. **Muhammad Farhan Ali Khan**: Investigation, Formal analysis. **Kifayat Ullah Shah**: Conceptualization, Supervision, Writing- Reviewing and Editing. **Abbas Rahdar:** Conceptualization, Supervision, Writing- Reviewing and Editing. **Ana M. Díez-Pascual:** Supervision, Writing- Reviewing and Editing.

Declaration of competing interest

The authors declare that they have no known competing financial interests or personal relationships that could have appeared to influence the work reported in this paper.

Data availability

The data required for reproduction of the provided work and research in the current paper are available upon contacting the corresponding author.

References

[1] G.S. Hussey, J.L. Dziki, S.F. Badylak, Extracellular matrix-based materials for regenerative medicine, Nat. Rev. Mater. 3 (2018) 159–173, https://doi.org/10.1038/s41578-018-0023-x.
[2] Y.X.J. Wáng, B.C. Lentle, Radiographic osteoporotic vertebral fractures in elderly men: a brief review focusing on differences between the sexes, Quant. Imaging Med. Surg. 10 (2020) 1863–1876, https://doi.org/10.21037/qims-2020-21.
[3] M.T. Chibuzor, D. Graham-Kalio, J.O. Osaji, M.M. Meremikwu, Vitamin D, calcium or a combination of vitamin D and calcium for the treatment of nutritional rickets in children, Cochrane Database Syst. Rev. 4, N. pag (2020), https://doi.org/10.1002/14651858.CD012581.pub2.
[4] S. Congedi, C. Minotti, C. Giaquinto, L. Da Dalt, D. Donà, Acute infectious osteomyelitis in children: new treatment strategies for an old enemy. World journal of pediatrics world, J. Pediatr. 16 (2020) 446–455, https://doi.org/10.1007/s12519-020-00359-z.
[5] H.K. Bhattarai, S. Shrestha, K. Rokka, R. Shakya, Vitamin D, calcium, parathyroid hormone, and sex steroids in bone health and effects of aging, J. Osteoporos. (2020), https://doi.org/10.1155/2020/9324505, 2020, N. pag.
[6] R. Chapurlat, M.A. Legrand, Bisphosphonates for the treatment of fibrous dysplasia of bone, Bone 143 (2021), 115784, https://doi.org/10.1016/j.bone.2020.115784.
[7] P. Kazimierczak, K. Palka, A. Przekora, Development and optimization of the novel fabrication method of highly macroporous chitosan/agarose/nanohydroxyapatite bone scaffold for potential regenerative medicine applications, Biomolecules. 9 (2019) 434, https://doi.org/10.3390/biom9090434.
[8] G. Hassan, S.M. Afify, S. Kitano, A. Seno, H. Ishii, Y. Shang, M. Matsusaki, M. Seno, Cancer stem cell microenvironment models with biomaterial scaffolds in vitro, Processes 9 (2020) 45, https://doi.org/10.3390/pr9010045.
[9] P. Vahedi, R. Moghaddamshahabi, T.J. Webster, A.C. Calikoglu Koyuncu, E. Ahmadian, W.S. Khan, A. Jimale Mohamed, A. Eftekhari, The use of infrapatellar fat pad-derived mesenchymal stem cells in articular cartilage regeneration: a review, Int. J. Mol. Sci. 22 (2021) 9215, https://doi.org/10.3390/ijms22179215.
[10] K. Khezri, S. Maleki Dizaj, Y. Rahbar Saadat, S. Sharifi, S. Shahi, E. Ahmadian, A. Eftekhari, E. Dalir Abdolahinia, F. Lotfipour, Osteogenic differentiation of mesenchymal stem cells via curcumin-containing nanoscaffolds, Stem Cells intl. 2021 (2021), https://doi.org/10.1155/2021/1520052.
[11] S. Vedovatto, J.C. Facchini, R.K. Batista, T.C. Paim, M.I.Z. Lionzo, M.R. Wink, Development of chitosan, gelatin and liposome film and analysis of its biocompatibility in vitro, Intl J. Biol. Macromol. 160 (2020) 750–757, https://doi.org/10.1016/j.ijbiomac.2020.05.229.
[12] A. Bakopoulou, A. Georgopoulou, I. Grivas, C. Bekiari, O. Prymak, K. Loza, M. Epple, G.C. Papadopoulos, P. Koidis, M. Chatzinikolaidou, Dental pulp stem cells in chitosan/gelatin scaffolds for enhanced orofacial bone regeneration, Dent. Mater. J. 35 (2019) 310–327, https://doi.org/10.1016/j.dental.2018.11.025.
[13] H. Chi, X. Song, C. Song, W. Zhao, G. Chen, A. Jiang, X. Wang, T. Yu, L. Zheng, J. Yan, Chitosan-gelatin scaffolds incorporating decellularized platelet-rich fibrin promote bone regeneration, ACS Biomater. Sci. Eng. 5 (2019) 5305–5315, https://doi.org/10.1021/acsbiomaterials.9b00788.
[14] F. Tao, Y. Cheng, X. Shi, H. Zheng, Y. Du, W. Xiang, H. Deng, Applications of chitin and chitosan nanofibers in bone regenerative engineering, Carbohydr. Polym. 230 (2020), 115658, https://doi.org/10.1016/j.carbpol.2019.115658.
[15] A.B. Bello, D. Kim, D. Kim, H. Park, S.-H. Lee, Engineering and functionalization of gelatin biomaterials: from cell culture to medical applications, Tissue Eng. Part B Rev. 26 (2020) 164–180, https://doi.org/10.1089/ten.teb.2019.0256.
[16] R. Naomi, H. Bahari, P.M. Ridzuan, F. Othman, Natural-based biomaterial for skin wound healing (Gelatin vs. collagen), Expert. rev. Polymers 13 (2021) 2319, https://doi.org/10.3390/polym13142319.
[17] M. Usman, A. Sahar, M. Inam-Ur-Raheem, U.U. Rahman, A. Sameen, R.M. Aadil, Gelatin extraction from fish waste and potential applications in food sector, Int. J. Food Sci. Technol. 57 (2022) 154–163, https://doi.org/10.1111/ijfs.15286.
[18] M. Efstathiou, L. Settas, The effect of non-steroidal anti-inflammatory drugs on matrix metalloproteinases levels in patients with osteoarthritis, Mediterr. J. Rheumatol 28 (2017) 133–141, https://doi.org/10.31138/mjr.28.3.133.
[19] S. Sharma, S. Tiwari, A review on biomacromolecular hydrogel classification and its applications, Int. J. Biol. Macromol. 162 (2020) 737–747, https://doi.org/10.1016/j.ijbiomac.2020.06.110.
[20] D.S. Malik, G. Kaur, Nanostructured gel for topical delivery of azelaic acid: designing, characterization, and in-vitro evaluation, J. Drug. Deliv. Sci. Technol. 47 (2018) 123–136, https://doi.org/10.1016/j.jddst.2018.07.008.
[21] A.A. El-Fattah, A. Mansour, Viscoelasticity, mechanical properties, and in vitro biodegradation of injectable chitosan-poly (3-hydroxybutyrate-co-3-hydroxyvalerate)/nanohydroxyapatite composite hydrogel, Bull. Mater. Sci. 41 (2018) 1–10, https://doi.org/10.1007/s12034-018-1663-6.
[22] L. Fan, H. Yang, J. Yang, M. Peng, J. Hu, Preparation and characterization of chitosan/gelatin/PVA hydrogel for wound dressings, Carbohydr. Polym. 146 (2016) 427–434, https://doi.org/10.1016/j.carbpol.2016.03.002.
[23] S. Kumbhar, V. Matole, Y. Thorat, S. Madur, S. Patil, A. Shegaonkar, Formulation and evaluation of lignocaine hydrochloride topical gel, Research J. Pharm. and Tech. 14 (2021) 908–910, https://doi.org/10.5958/0974-360X.2021.00161.X.
[24] F. Sabir, M.I. Asad, M. Qindeel, I. Afzal, M.J. Dar, K.U. Shah, A. Zeb, G.M. Khan, N. Ahmed, F.-U. Din, Polymeric nanogels as versatile nanoplatforms for biomedical applications, J. Nanomater. (2019), https://doi.org/10.1155/2019/1526186.

[25] I. Guideline, Stability testing of new drug substances and products. Q1A (R2), current step 4, 2003 (1-24).
[26] H. Yuan, X. Zheng, W. Liu, H. Zhang, J. Shao, J. Yao, C. Mao, J. Hui, D. Fan, A novel bovine serum albumin and sodium alginate hydrogel scaffold doped with hydroxyapatite nanowires for cartilage defects repair, Colloids Surf. B: Biointerfaces 192 (2020), 111041, https://doi.org/10.1016/j.colsurfb.2020.111041.
[27] S. Bhattacharjee, DLS and zeta potential–what they are and what they are not? J. Control. Release 235 (2016) 337–351, https://doi.org/10.1016/j.jconrel.2016.06.017.
[28] V.M. Esquerdo, P.P. Silva, G.L. Dotto, L.A. Pinto, Nanoemulsions from unsaturated fatty acids concentrates of carp oil using chitosan, gelatin, and their blends as wall materials, Eur. J. Lipid Sci. Technol. 120 (2018) 1700240, https://doi.org/10.1002/ejlt.201700240.
[29] M. Das, P. Suguna, K. Prasad, J. Vijaylakshmi, M. Renuka, Extraction and characterization of gelatin: a functional biopolymer, Int J Pharm Pharm Sci 9 (2017) 239–242, https://doi.org/10.22159/ijpps.2017v9i9.17618.
[30] A. Mahmoud, O. Osman, K. Eid, E. Ashkar, A. Okasha, D. Atta, M. Eid, Z. Aziz, A. Fakhry, FTIR spectroscopy of natural bio-polymers blends, Middle East. J. Appl. Sci 4 (2014) 816–824. Corpus ID: 106211891.
[31] D. Pradini, H. Juwono, K.A. Madurani, F. Kurniawan, A preliminary study of identification halal gelatin using quartz crystal microbalance (QCM) sensor, MJFAS 14 (3) (2018) 325–330, https://doi.org/10.11113/mjfas.v14n3.942.
[32] H. Rahim, A. Sadiq, R. Ullah, A. Bari, F. Amin, U. Farooq, N.U. Jan, H. M. Mahmood, Formulation of aceclofenac tablets using nanosuspension as granulating agent: an attempt to enhance dissolution rate and oral bioavailability, Int. J. Nanomedicine 15 (2020) 8999–9009, https://doi.org/10.2147/IJN.S270746.
[33] K. Phogat, S. Bandyopadhyay-Ghosh, Nanocellulose mediated injectable bio-nanocomposite hydrogel scaffold-microstructure and rheological properties, Cellulose 25 (2018) 5821–5830, https://doi.org/10.1007/s10570-018-2001-2.
[34] S. İlk, A. Ramanauskaitė, B.K. Bilican, P. Mulerčikas, D. Cam, M.S. Onses, I. Torun, S. Kazlauskaitė, V. Baublys, Ö. Aydın, Usage of natural chitosan membrane obtained from insect corneal lenses as a drug carrier and its potential for point of care tests, Mater. Sci. Eng. C. 112 (2020), 110897, https://doi.org/10.1016/j.msec.2020.110897.
[35] S. Jana, A. Saha, A.K. Nayak, K.K. Sen, S.K. Basu, Aceclofenac-loaded chitosan-tamarind seed polysaccharide interpenetrating polymeric network microparticles, Colloids Surf B Biointerfaces. 105 (2013) 303–309, https://doi.org/10.1016/j.colsurfb.2013.01.013.
[36] C.M. Murphy, M.G. Haugh, F.J. O'brien, The effect of mean pore size on cell attachment, proliferation and migration in collagen–glycosaminoglycan scaffolds for bone tissue engineering, Biomaterials. 31 (2010) 461–466, https://doi.org/10.1016/j.biomaterials.2009.09.063.
[37] K. Rajamäki, T. Nordström, K. Nurmi, K.E. Åkerman, P.T. Kovanen, K. Öörni, K. K. Eklund, Extracellular acidosis is a novel danger signal alerting innate immunity via the NLRP3 inflammasome, J. Biol. Chem. 288 (2013) 13410–13419, https://doi.org/10.1074/jbc.M112.426254.
[38] S.A. Islam, S. Islam, M. Shahriar, I. Dewan, Comparative in vitro dissolution study of aceclofenac marketed tablets in two different dissolution media by validated analytical method, J App Pharm Sci. ISSN: 2231-3354 1 (2011) 87–92.
[39] N. Abbasi, S. Hamlet, R.M. Love, N.-T. Nguyen, Porous scaffolds for bone regeneration, J Sci-Adv Mater Dev. 5 (2020) 1–9, https://doi.org/10.1016/j.jsamd.2020.01.007.
[40] V. Karageorgiou, D. Kaplan, Porosity of 3D biomaterial scaffolds and osteogenesis, Biomaterials 26 (2005) 5474–5491, https://doi.org/10.1016/j.biomaterials.2005.02.002.
[41] T. Dutta Roy, J.L. Simon, J.L. Ricci, E.D. Rekow, V.P. Thompson, J.R. Parsons, Performance of hydroxyapatite bone repair scaffolds created via three-dimensional fabrication techniques, J Biomed Mater Res A: An Official Journal of The Society for Biomaterials, The Japanese Society for Biomaterials, and The Australian Society for Biomaterials and the Korean Society for Biomaterials. 67 (2003) 1228–1237, https://doi.org/10.1002/jbm.a.20034.
[42] J. Will, R. Melcher, C. Treul, N. Travitzky, U. Kneser, E. Polykandriotis, R. Horch, P. Greil, Porous ceramic bone scaffolds for vascularized bone tissue regeneration, J Mater Sci Mater Med. 19 (2008) 2781–2790, https://doi.org/10.1007/s10856-007-3346-5.
[43] L. Kong, Q. Ao, A. Wang, K. Gong, X. Wang, G. Lu, Y. Gong, N. Zhao, X. Zhang, Preparation and characterization of a multilayer biomimetic scaffold for bone tissue engineering, J. Biomater. Appl. 22 (2007) 223–239, https://doi.org/10.1177/0885328206073706.
[44] M. Vigata, C. Meinert, D.W. Hutmacher, N. Bock, Hydrogels as drug delivery systems: a review of current characterization and evaluation techniques, Pharmaceutics 12 (2020) 1188, https://doi.org/10.3390/pharmaceutics12121188.
[45] J. Li, D.J. Mooney, Designing hydrogels for controlled drug delivery, Nat. Rev. Mater. 1 (2016) 1–17, https://doi.org/10.1038/natrevmats.2016.71.
[46] K.G. Nairon, T. DePalma, H. Sivakumar, A. Skardal, in: Controlled Drug Delivery Systems, CRC Press, Boca Raton, FL, USA, 2020, pp. 29–53. Chapter 3. Tunable Hydrogel Systems for Delivery and Release of Cell-Secreted and Synthetic Therapeutic Products.
[47] B. Kaczmarek, A. Sionkowska, M. Gołyńska, I. Polkowska, T. Szponder, D. Nehrbass, A. Osyczka, In vivo study on scaffolds based on chitosan, collagen, and hyaluronic acid with hydroxyapatite, Int. J. Biol. Macromol. 118 (2018) 938–944, https://doi.org/10.1016/j.ijbiomac.2018.06.175.
[48] S.S. Panchal, D.V. Vasava, Biodegradable polymeric materials: synthetic approach, ACS omega 5 (2020) 4370–4379, https://doi.org/10.1021/acsomega.9b04422.
[49] H.C. Tan, Is a biodegradable polymer stent really superior to a durable polymer stent? Www, asiaintervention.org. (2018) 71, https://doi.org/10.4244/AIJV4I2A14.
[50] S. Ghosh, D. Lahiri, M. Nag, A. Dey, T. Sarkar, S.K. Pathak, H. Atan Edinur, S. Pati, R.R. Ray, Bacterial Biopolymer: Its Role in Pathogenesis to Effective Biomaterials, Polymers 13 (1242) (2021), https://doi.org/10.3390/polym13081242.
[51] A. Mahmood, D. Patel, B. Hickson, J. DesRochers, X. Hu, Recent Progress in biopolymer-based hydrogel materials for biomedical applications, Int. J. Mol. Sci. 23 (2022) 1415, https://doi.org/10.3390/ijms23031415.
[52] F. Mo, K. Jiang, D. Zhao, Y. Wang, J. Song, W. Tan, DNA hydrogel-based gene editing and drug delivery systems, Adv. Drug Deliv. Rev. 168 (2021) 79–98, https://doi.org/10.1016/j.addr.2020.07.018.
[53] Patra, et al., Nano based drug delivery systems: recent developments and future prospects, J. Nanobiotechnol. 16 (2018) 71, https://doi.org/10.1186/s12951-018-0392-8.
[54] A.A. Date, J. Hanes, L.M. Ensign, Nanoparticles for oral delivery: design, evaluation and state-of-the-art, J. Control. Release 240 (2016) 504–526, https://doi.org/10.1016/j.jconrel.2016.06.016.